Effect of CT-based attenuation correction on uptake ratios in skeletal SPECT

Effekt der CT-basierten Schwächungskorrektur auf den Uptake im Skelett-SPECT

V. Schulz[1], I. Nickel[1], A. Nömayr[1], A. H. Vija[2], C. Hocke[1], J. Hornegger[3], W. Bautz[4], W. Römer[1], T. Kuwert[1]
[1]Clinic of Nuclear Medicine, [3]Chair of Pattern Recognition, [4]Institute of Diagnostic Radiology, University of Erlangen/ Nürnberg, Erlangen, Germany
[2]Siemens Medical Solutions, Molecular Imaging, SPECT Research, Hoffman Estates, USA

Keywords
SPECT/ CT, image fusion, hybrid imaging, attenuation correction, bone scintigraphy

Summary
The **aim** of this study was to determine the clinical relevance of compensating SPECT data for patient specific attenuation by the use of CT data simultaneously acquired with SPECT/CT when analyzing the skeletal uptake of polyphosphonates (DPD). Furthermore, the influence of misregistration between SPECT and CT data on uptake ratios was investigated. **Methods:** Thirty-six data sets from bone SPECTs performed on a hybrid SPECT/CT system were retrospectively analyzed. Using regions of interest (ROIs), raw counts were determined in the fifth lumbar vertebral body, its facet joints, both anterior iliacal spinae, and of the whole transversal slice. ROI measurements were performed in uncorrected (NAC) and attenuation-corrected (AC) images. Furthermore, the ROI measurements were also performed in AC scans in which SPECT and CT images had been misaligned by 1 cm in one dimension beforehand (ACX, ACY, ACZ). **Results:** After AC, DPD uptake ratios differed significantly from the NAC values in all regions studied ranging from 32% for the left facet joint to 39% for the vertebral body. AC using misaligned pairs of patient data sets led to a significant change of whole-slice uptake ratios whose differences ranged from 3,5 to 25%. For ACX, the average left-to-right ratio of the facet joints was by 8% and for the superior iliacal spines by 31% lower than the values determined for the matched images ($p < 0.05$). **Conclusions:** AC significantly affects DPD uptake ratios. Furthermore, misalignment between SPECT and CT may introduce significant errors in quantification, potentially also affecting left-to-right ratios. Therefore, at clinical evaluation of attenuation-corrected scans special attention should be given to possible misalignments between SPECT and CT.

Nuklearmedizin 2007; 46: 38–42

Schlüsselwörter
SPECT/CT, Bildfusion, Hybridbildgebung, Schwächungskorrektur, Knochenszintigraphie

Zusammenfassung
Ziel dieser Studie war es, die klinische Relevanz der Schwächungskorrektur von SPECT-Daten im Rahmen der Skelettszintigraphie herauszufinden. Für die Schwächungskorrektur wurden mittels SPECT/CT gewonnene CT-Daten verwendet. Zusätzlich wurde der Einfluss einer Verschiebung zwischen SPECT- und CT-Datensatz auf die DPD-Uptake-Verhältnisse untersucht. **Methoden:** Die Datensätze von 36 DPD-SPECTs wurden analysiert, die an einem SPECT/CT-Hybridsystem erhoben worden waren. Unter Verwendung von ROIs (regions of interest) wurden die Zählraten im fünften Lendenwirbelkörper, dessen Facettengelenken, den beiden Spinae iliacae ant. sup. und der gesamten transversalen Schicht bestimmt. Für die Messungen wurden die unkorrigierten (NAC) und schwächungskorrigierten (AC) Bilder verwendet. Außerdem erfolgten ROI-Messungen an schwächungskorrigierten Datensätzen, bei denen vor der Schwächungskorrektur die SPECT- und CT-Daten manuell um 1 cm gegeneinander in einer Dimension verschoben worden waren (ACX, ACY, ACZ). **Ergebnisse:** Die schwächungskorrigierten Uptake-Verhältnisse von DPD unterschieden sich in allen ausgewerteten Regionen signifikant von den unkorrigierten Werten. Die prozentuale Abweichung reichte von 32% im linken Facettengelenk bis 39% im Wirbelkörper. Eine Schwächungskorrektur, die mit verschobenen Datenpaaren durchgeführt wurde, führte zu einer signifikanten Änderung der Uptake-Verhältnisse der gesamten Schicht im Bereich von 3,5-25%. Für ACX war der durchschnittliche Links/Rechts-Quotient der Facettengelenke um 8% und der der Spinae iliacae ant. sup. um 31% niedriger als die Werte, die für optimal registrierte Datensätze gemessen wurden ($p < 0,05$). **Schlussfolgerung:** Die Schwächungskorrektur beeinflusst DPD-Uptake-Verhältnisse in signifikanter Weise. Außerdem kann eine Verschiebung zwischen SPECT und CT signifikante Fehler in der Quantifizierung bewirken und potenziell die Links/Rechts-Quotienten verändern. Bei der klinischen Auswertung von schwächungskorrigierten Daten sollte deshalb speziell auf mögliche Verschiebungen zwischen SPECT und CT geachtet werden.

The functional imaging modality single-photon emission computed tomography (SPECT) allows the visualization and measurement of molecular processes in vivo. However, it suffers from low spatial resolution when compared to X-ray computed tomography (CT) or magnetic resonance imaging (MRI). Therefore, foci of tracer uptake may be difficult to localize using these techniques, leading to a deterioration of their diagnostic accuracy.

One way to improve diagnostic accuracy of SPECT is to register images from this modality to those from CT and MRI. This may be performed using software registration on data sets acquired on stand-alone devices. A multitude of studies have proven this approach to be of clinical value (6-8, 13, 18, 20, 22, 31, 32). A shortcoming of software-based image fusion is its anatomical inaccuracy which has been described to range between about 0.5 to 2 cm, depending on the modalities matched, the approach used, and the localization of the lesions studied (10, 22, 23). In addition to inaccuracies inherent to the process of registration, movements of the patient between both examinations and their different positioning on the different scanner beds account for the misalignment of image pairs registered post hoc (22).

Hardware-based image registration has become possible by the development of hybrid systems integrating detectors from different modalities within one gantry. This approach was first realized for PET/CT (38) and has been met with great acceptance in the field (2). With these systems, the anatomical inaccuracies of image fusion are expected to be much reduced compared to software-based post hoc image fusion, although inaccuracies in the thorax due to respiratory movements still prevail (5, 21, 22).

Received: August 17, 2006; accepted in revised form: October 17, 2006

Seven years ago, a hybrid system combining a dual-headed SPECT camera with a non-diagnostic computerized tomographical scanner (CT) has been introduced (1, 24, 35, 37). Several studies evidence its clinical value (29, 30, 33). Especially for bone scintigraphy, Horger et al. (16) recently demonstrated that the use of this type of camera improves diagnostic specificity with regard to differentiating benign from malignant lesions to the bone. Nevertheless, a shortcoming of these systems is the limited resolution of their CT component, potentially obviating the detection of small benign or neoplastic lesions.

In 2005, a spiral-CT scanner offering todate diagnostic performance of CT and a SPECT camera were integrated within the same gantry. Evidence reporting the clinical performance of SPECT/spiral-CT is still scarce. However, it has, in particular, been shown that SPECT/spiral-CT considerably improves the diagnostic accuracy of radionuclide bone scanning in staging tumour patients (27, 39).

SPECT/CT systems with a common patient bed allow for SPECT and CT acquisitions without the patient having to move and thus limiting misalignment between the two data sets caused by differences in patient positioning. The average registration inaccuracy using integrated SPECT/CT systems in the lower lumbar spine has been shown to be in the range of 1-1.5 mm and thus well below pixel width in the majority of cases (23).

CT data can also be used to compensate for attenuation in SPECT as previously shown (26). In this process, the Hounsfield units are converted to linear attenuation coefficients at the emission energy of the isotope used. A pixel-by-pixel conversion is used, where a patient specific effective CT transmission energy is estimated from the CT data, and then converted to linear attenuation coefficients. The resulting attenuation-corrected data are expected to give a more accurate image of the distribution of radioactivity within the patient's body. In a previous study, we showed that CT-based attenuation correction homogenizes the SPECT image of a cylindrical phantom filled with ^{111}In and also the visualization of the liver in patients examined using ^{111}In-octreotide (26).

As yet, no data on the effect of CT-based attenuation correction of uptake ratios of ^{99m}Tc-polyphosphonates (DPD) have been published. Therefore, the aim of this study was to analyze the effect of CT-based attenuation correction on these variables determined in bone SPECT. Furthermore, we sought to determine the effect of misalignments between SPECT and CT on these variables.

Patients, material, methods

Patients

A set of 36 patients was selected for this study, from patients examined by skeletal SPECT/spiral-CT involving the lower lumbar spine between March and August 2005. It consisted of 23 women and 13 men, mean age was 66 years. All patients had been examined for clinical reasons. The indications were

- breast cancer in 17 cases,
- arthrosis in four cases,
- intestinal cancer in three cases,
- prostate and bladder cancer in two cases,
- lung and prostate cancer in one case each,
- lung and bladder cancer in one case,
- osteolytic tumour, lymphoma, granuloma in one case each,
- spondylodiscitis, slipped disc, sacrum fracture, lower back pain in one case each.

Data acquisition and reconstruction

Three hours after intravenous injection of 7-10 MBq/kg body weight ^{99m}Tc-diphosphonate planar whole body scintigraphies were performed using a dual-headed gamma-camera (e-cam; Siemens Medical Solutions, Erlangen). SPECT/spiral-CT was performed 3-4 hours after tracer injection using hybrid SPECT/CT (Symbia T2, Siemens Medical Solutions, Erlangen).

The SPECT was performed with a field of view from the ischiadic tuber to Th12/L1. The field of view of the CT was limited to the pelvis including L4/L5 in all cases. As reported previously, the details of data acquisition and reconstruction were the following:

For SPECT, counts from the 15% energy windows at 140 keV were acquired into a 128 × 128 matrix leading to a pixel size of 4.8 × 4.8 mm. A total of 64 frames, each of a duration of 30 s, were acquired over 360°. The camera heads were equipped with high-resolution low-energy parallel-hole collimators (LEHR) (27).

The scan parameters for the CT were the following: 130 kV; reference dose 20 mAs with real-time tube current modulation (CARE Dose4D), Siemens Medical Solutions, Erlangen, Germany) to minimize patient dose; rotation time 0.8 s; collimation 2 × 2.5 mm. Image reconstruction resulted in images with a slice thickness of 3 mm using a 1.5 mm reconstruction increment. Both the SPECT and the CT scans were performed consecutively with the patient lying stable in a supine position with elevated arms.

SPECT and CT data were transferred to the e.soft processing workstation. Raw SPECT data were reconstructed into transaxial slices using the e.soft reconstruction software. Reconstruction was performed iteratively by using the ordered subsets expectation maximization (OSEM 3D) technique with 4 iterations and 8 subsets, allowing for isotropic spatial resolution of the reconstructed images (28). Images were post-smoothed with a 3D spatial Gaussian filter (FWHM 8.40 mm).

For attenuation correction, the CT data sets were integrated into the process of reconstruction. These data were closely matched to the SPECT data due to hardware-based image fusion. In addition, an automated rigid software fusion provided by the manufacturer (image registration activity; e.soft 5.0) was performed to further minimize registration error, if possible.(23). All data pairs were visually checked for misalignment. Deviations of more than 5 mm were not detected. When assessing effects of misalignment, the optimally registered data pairs were interactively misaligned by 1 cm in each of the three dimensions using the image registration activity of e.soft 5.0.

Attenuation correction was automated using the activities implemented in the e.soft

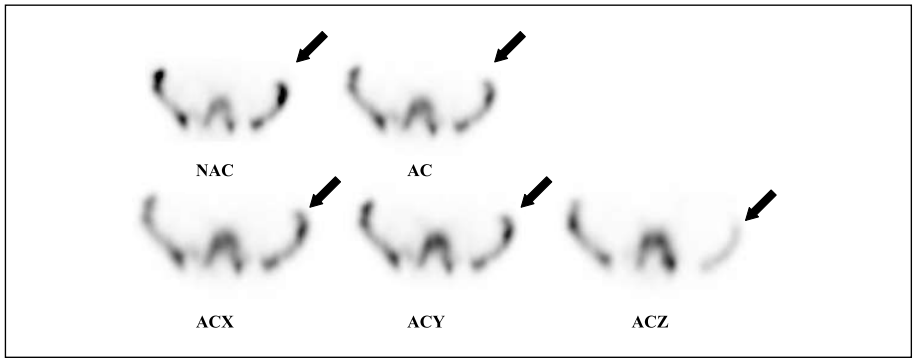

Fig. 1 Effects of attenuation correction in a transversal SPECT scan in a representative patient (NAC: no attenuation correction; AC: attenuation-corrected SPECT scan using an aligned CT data set; ACX: attenuation corrected SPECT using a CT data set misaligned by 1 cm in X-direction; ACY: attenuation corrected SPECT using a CT data set misaligned by 1 cm in Y-direction; ACZ: attenuation corrected SPECT using a CT data set misaligned by 1 cm in Z-direction). Arrow indicates marked changes in visualization of tracer uptake.

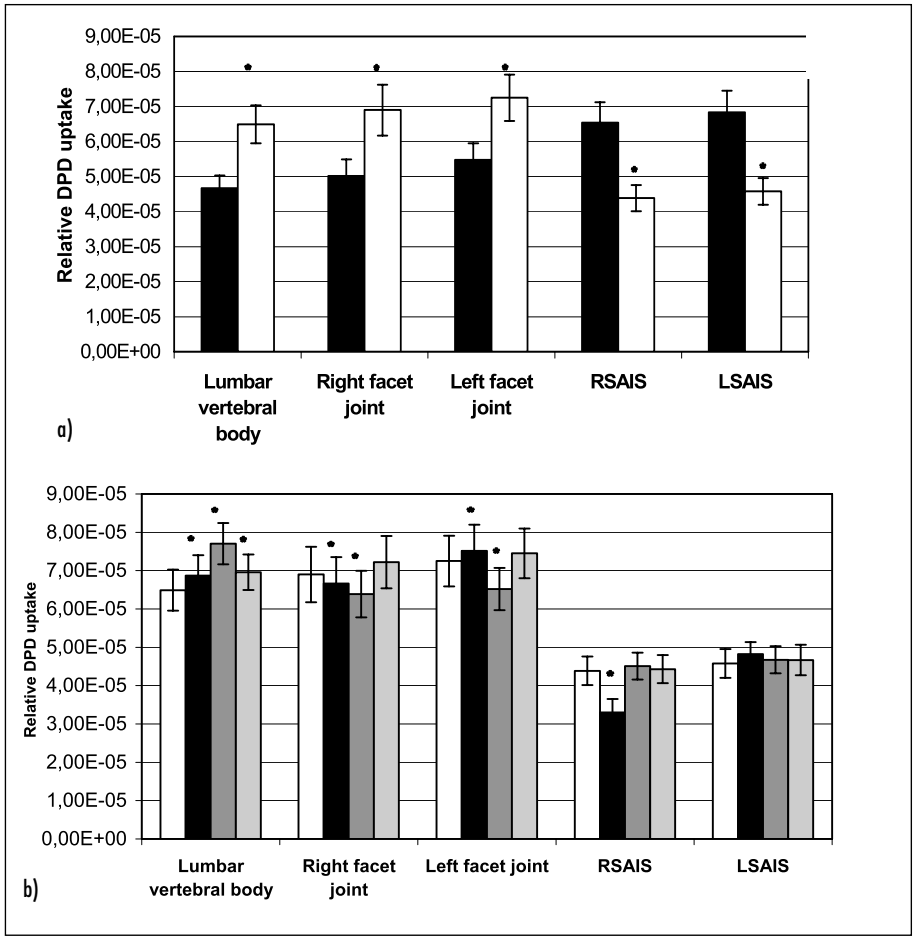

Fig. 2 DPD uptake ratios in several regions-of-interest determined in 36 patients
RSAIS (LSAIS): right (left) superior anterior iliac spine; bars: standard errors of the mean
a) □: data from attenuation-corrected scans (AC); ■: data from uncorrected images (NAC); *$p < 0.01$
b) □: data from attenuation-corrected and optimally aligned data sets (AC); ■: data from pairs of SPECT and CT misaligned by 1 cm in X-direction (ACX); ■: data from image pairs misaligned by 1 cm in Y-direction (ACY); ■: data from image pairs misaligned by 1 cm in Z-direction (ACZ); *$p < 0.02$

software (attenuation map activity, tomo reconstruction activity). The attenuation correction method used in our study includes the attenuation in the forward as well as backward projections (bilinear attenuation correction) of the implemented OSEM 3D reconstruction. Therefore, this bilinear attenuation correction is not a multiplicative correction. Scatter correction was indirectly considered by utilizing a broad beam model in the reconstruction, where attenuation values are reduced by some factor compared to the theoretical ones. Generally, this factor depends on the energy of the tracer and the acquisition window width. In our studies, the default factor for ^{99m}Tc given by the manufacturer was 0.7632. The attenuation-corrected and the non-corrected data were reconstructed with identical parameters. The above-described process resulted in five SPECT data sets for each patient (NAC, AC, ACX, ACY, ACZ).

A transversal slice transecting the body of the fifth lumbar vertebra was chosen for further analysis. This slice included the anterior superior iliac spinae in all cases. Irregular regions of interest (ROIs) covering the vertebral body, its facet joints, and the superior anterior iliac spines were defined on the optimally fused CT and then transferred to the SPECT images using the e.soft volumetric analysis activity. In the SPECT images which were reconstructed by the use of a misaligned CT, the positioning of the ROIs was identical to that on the original, optimally fused data sets, since the position of the SPECT dataset with regard to the optimally matched CT was not changed by the attenuation correction performed with the misaligned CT.

For the vertebral body, the facet joints, and the spinae, the average uptake in the ROI was used; these values were divided by the total counts within the slice as reference.

Phantom study

For the phantom study, a cylindrical phantom (PTW acc IEC 61675–1) with rod inserts filled with ^{99m}Tc was used. The radioactivity concentrations for the two fillable rods were 167 and 333 kBq/ml, respectively. The large volume of the cylindrical phan-

tom was left empty. SPECT acquisition was performed using a 128 × 128 matrix and 64 views for a 360° rotation. 50 kcts/view were collected. The data was corrected for attenuation and scatter within an iterative OSEM 3D reconstruction. A circular ROI was defined in the rod filled with the lower radioactivity concentration. ROI measurements were performed in non-attenuation corrected (NAC) and attenuation-corrected (AC) images as well as AC scans in which SPECT and CT images had been misaligned by 1 cm and 2 cm in one dimension beforehand (ACX, ACY, ACZ) similar to the procedure in the patients' data sets.

Furthermore, linear ROIs were drawn on ten central slices with and without attenuation correction and misalignment to allow for the display of line profiles.

Data analysis

The significance of differences in relative uptake values was tested using the non-parametric Wilcoxon-test. The level of significance was set at $p < 0.05$. Bonferroni´s correction was used in the case of multiple comparisons. All data are given as mean value ± standard error of the mean unless otherwise specified.

Results

Figure 1 provides representative images for one of the patients studied, illustrating the effects of attenuation correction and the artefacts produced by the misalignment between the CT and SPECT image data sets. The efficiency of the CT-based attenuation correction applied herein is demonstrated in Figure 1. In contrast to the uncorrected image, a more homogeneous tracer distribution is visible after attenuation correction. Uptake ratios are increased in the central regions and decreased in the iliac spines, which are situated in the periphery.

Whole-slice ratios of DPD uptake determined on attenuation-corrected images differed significantly from the values determined in uncorrected images in all regions investigated (Fig. 2a); the mean percentage differences ranged from 32% for the left facet joint to 39% for the vertebral body.

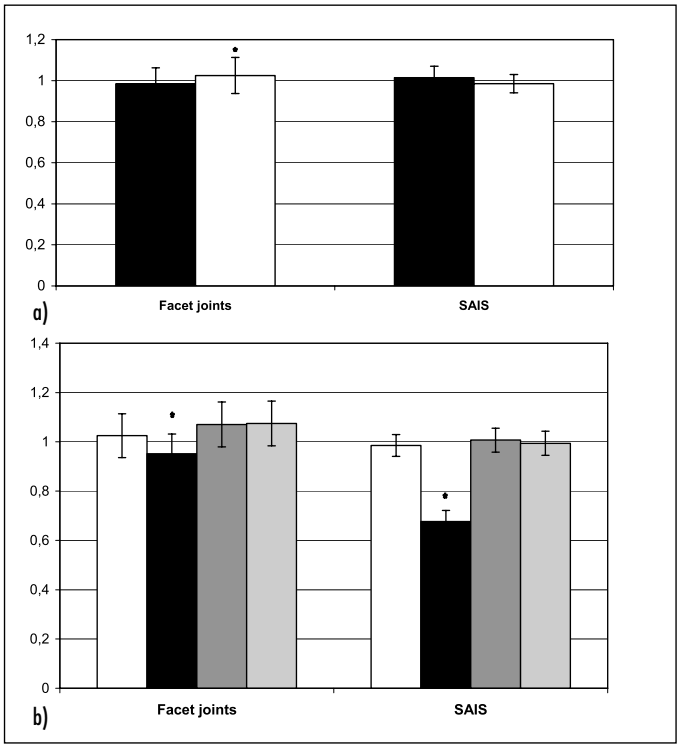

Fig. 3
Left-to-right ratios of DPD uptake in the facet joints and the superior anterior iliac spines (SAIS) determined in 36 patients (bars: standard errors of the mean); data from
a) □: attenuation-corrected SPECT images;
■: uncorrected scans;
*$p < 0.05$
b) □: attenuation-corrected and optimally aligned data sets (AC);
■: pairs of SPECT and CT misaligned by 1 cm in X-direction (ACX),
▒: image pairs misaligned by 1 cm in Y-direction (ACY);
▒: image pairs misaligned by 1 cm in Z-direction (ACZ);
*$p < 0.01$

Attenuation correction using misaligned pairs of patient data sets led to significant differences in whole-slice ratios when compared to attenuation-corrected images from well-aligned SPECT and CT: For misalignment in X-direction four of five, in Y-direction three of five, and in Z-direction one of five regions had either significantly lower (n = 4) or higher (n = 4) relative DPD uptake. The differences in uptake ratios between aligned and misaligned data sets ranged from 3.5 to 25% (Fig. 2b).

Left-to-right ratios were not affected by more than 5% by AC (Fig. 3a). Misalignment in Y- and Z-direction did not lead to significant differences in left-to-right ratios. However, misalignment of the datasets in X-direction produced left-to-right ratios significantly different from those from the perfectly matched data pairs (Fig. 3b). The difference was 8% for the facet joints and 31% for the superior iliacal spines.

Figure 4 demonstrates that, in the phantom study, CT misalignment by 1 cm and 2 cm in X- or Y-direction led to significant changes in count rate on the attenuation-corrected SPECT images, whereas misalignments in Z-direction did not produce any differences in this variable.

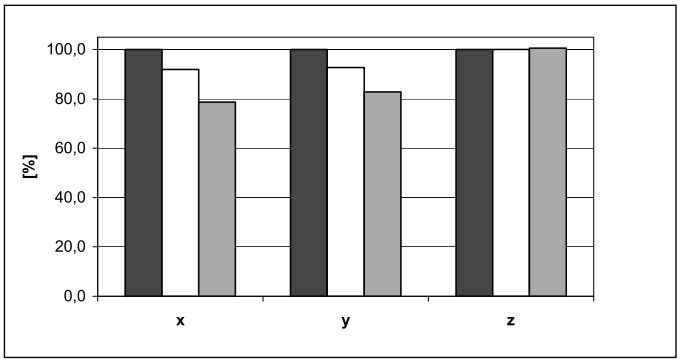

Fig. 4
Deviation in counts (%) caused by misalignment in the phantom study
■: 0 cm; □: 1 cm;
▒: 2 cm

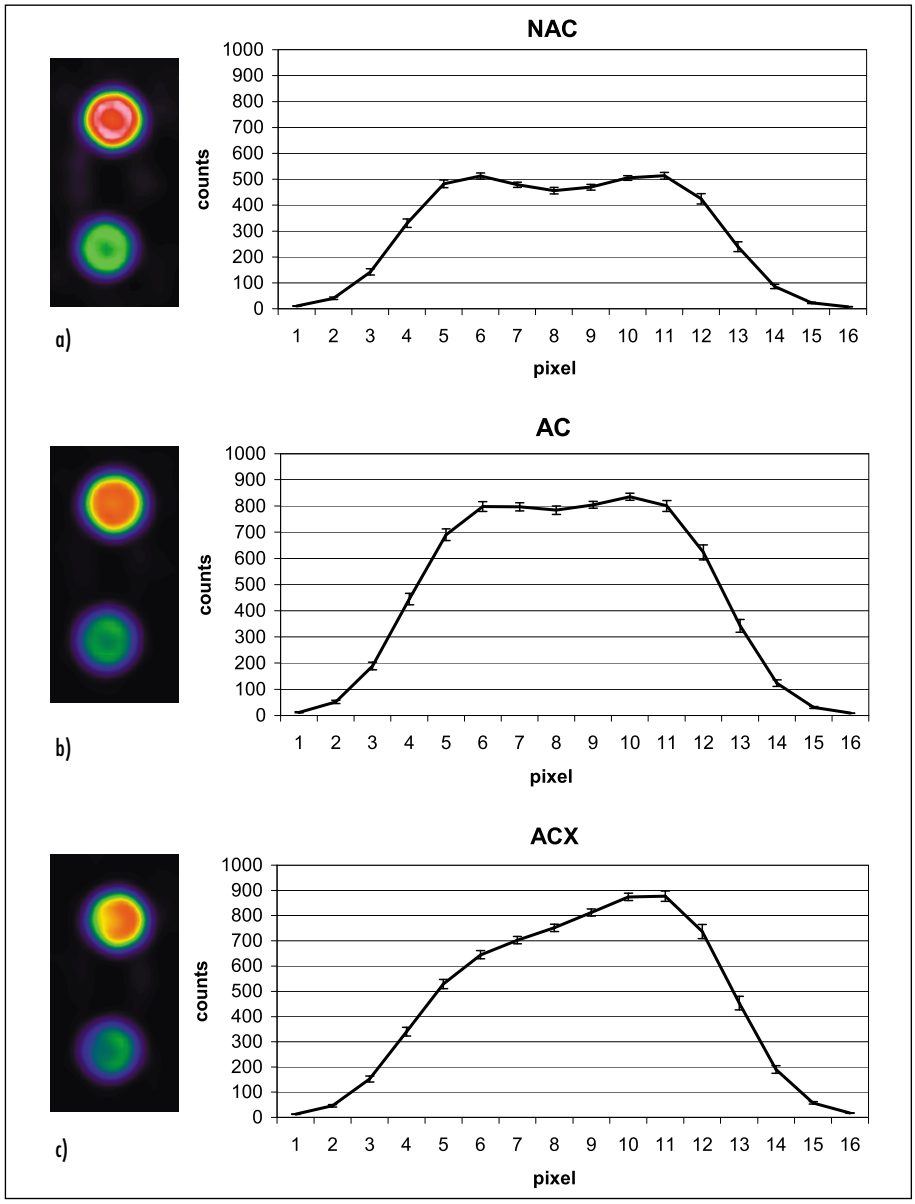

Fig. 5 Transversal SPECT images of a phantom filled with ^{99m}Tc
a) without (NAC) and b) with attenuation correction (AC); c) a CT misalignment by 1 cm in X-direction (ACX): improved homogeneity of tracer distribution after attenuation correction and inhomogeneity by using a misaligned CT for attenuation correction (curves: profiles from left to right for the rod filled with the lower radioactivity concentration in NAC, AC, and ACX)

In contrast to the uncorrected image, a homogeneous tracer distribution is reconstructed when performing CT-based attenuation correction (Fig. 5). In the images misaligned by 1 cm in each direction, reconstruction led to considerable inhomogeneity in tracer distribution. This visual impression is confirmed by the horizontal profiles crossing the homogeneously filled cylindrical phantom (Fig. 5).

Discussion

Clinical impact and relevance

The accuracy of SPECT in visualization and quantification of tissue tracer distribution is significantly affected by artefacts caused by photon attenuation. It was expected that CT-based attenuation correction led to significant changes of whole-slice ratios of DPD uptake in several regions of the pelvis and lower spine in our group of patients.

As to now, various methods of attenuation correction have been proposed (9, 15, 40). These may be subdivided into those with and those without transmission measurements. The former capitalize on the individual measurement of attenuation maps. The latter calculate tissue attenuation coefficients on the basis of an assumption of their distribution in the body segment examined, using various methods to determine the body outline. Most of these approaches have been developed to enable the attenuation-correction of SPECT studies of the brain or the heart.

In the brain, it is generally assumed that the attenuation coefficients are homogeneously distributed within this organ. Therefore, calculating attenuation coefficients using, e.g., the method introduced by Chang, is usually considered to be sufficient for clinical purposes (36). However, Stodilka et al.(34) have shown that the assumption of a homogeneous distribution of attenuation coefficients in the skull may lead to significant errors in the relative quantification of cerebral activity since this does not take non-uniformities in the attenuating effects of bone, scalp, the head-holder, and brain tissue into account. In their paper, errors of measurement ranged from 18 to 37% when Chang's attenuation correction was applied.

In SPECT studies of myocardial perfusion, attenuation artefacts do not only lead to errors in the quantification of tissue radioactivity concentration, but also to a reduction of diagnostic accuracy (19). Since the thorax contains tissues of variable attenuation, attenuation correction of myocardial scintigrams has to rely on individually measured data of attenuation. Various approaches for the determination of these attenuation maps have been proposed, mostly based on radionuclide transmission scanning. However, it has been repeatedly shown that the methods of attenuation correction using radionuclide transmission scanning can introduce artefacts that may be difficult to identify (4). A major problem inherent to these approaches is the low activity of the radioactive sources used leading either to long acquisition times or to attenuation maps with poor quality due to low counting rates.

This problem may be overcome when CT data registered to SPECT are employed for attenuation correction. Recently, Fricke and coworkers (11) have applied this method to SPECT images of myocardial perfusion and have compared its accuracy against to that of cardiac perfusion PET. They showed that the concordance between SPECT and PET studies of myocardial perfusion was improved after CT-based attenuation correction of SPECT.

We used a fast diagnostic capable CT for the attenuation-correction of our SPECT images. With this approach, whole-slice ratios of DPD uptake determined on attenuation-corrected images differed significantly from the values determined in uncorrected images in all regions investigated. The mean percentage differences ranged from 32% for the left facet joint to 40% for the vertebral body.

Evidence on the effect of attenuation correction on the visualization and quantification of the uptake of the radiolabeled polyphosphonates by the skeleton is scarce. Case and colleagues (3) compared three methods of correcting SPECT images of the cervical spine for attenuation artefacts. These were Chang's attenuation correction based on the interactive determination of the body outline either from the ^{99m}Tc emission photopeak data (ChangAC) or from emission data based on the downscatter of the ^{99m}Tc photons (ScatterAC) as well as attenuation correction based on a transmission measurement using a line source (TransAC). The latter two methods led to a significant improvement in the estimated cervical spine uptake, compared with either non-corrected scans or ChangAC. In the five patients studied by these authors, uptake ratios between midcervical and upper thoracic ROIs were corrected by approximately 40% by TransAC and ScatterAC, which is in the range of our data.

The uptake values reported herein are referred to DPD uptake of the whole transversal slice studied. This explains why relative uptake in the more superficially located regions, e.g., the iliac crest, decreased after attenuation correction, whereas relative uptake values in the vertebral body increased. This finding is in agreement with data we previously reported for relative uptake in metastases of neuroendocrine tumours studied with ^{111}In-octreotide-SPECT (26). In that study, the change in relative uptake caused by attenuation correction correlated significantly with the distance of the lesions from the surface of the body.

Effects of misalignment

Differences in the position of the patient caused by, e.g., patient movements between the acquisition of the SPECT and CT data, may lead to a misalignment between the images engendered by these two examinations. This may, in particular, be true when separately acquired image data sets are registered using software dedicated to image fusion (10). The average anatomical accuracy of hardware-based image fusion using a SPECT/ spiral-CT camera has been reported to be excellent in the lower spine (23). The occurrence of misalignment can, however, not be excluded in individual patients.

SPECT/CT misalignment may lead to errors in attenuation correction since emission voxels may be assigned a false attenuation coefficient voxel (4). In myocardial SPECT, misalignment between emission and transmission data by 7 mm, corresponding to the width of one pixel, was shown to produce a 15% change in relative regional activity (19). These results were recently reproduced for CT-based attenuation correction (12).

In our data, misalignment of the SPECT and CT data by 1 cm led to significant changes of DPD uptake ratios between 3.5 and 25%, corresponding in magnitude to those reported for myocardial SPECT. Of particular concern is that also left-to-right ratios were significantly influenced by misalignment since the assessment of symmetry in DPD uptake is one important criterion for interpreting bone-SPECT. As demonstrated for myocardial SPECT, misalignment between skeletal SPECT and CT data used for attenuation correction could therefore also lead to errors in clinical diagnoses. Therefore, the accuracy of SPECT/CT coregistration needs to be verified for every patient when attenuation-corrected SPECT scans are to be used for diagnostic purposes, even when using hybrid SPECT/CT devices.

In theory, a more realistic visualisation of the distribution of the tracer within the body of the patient should also be accompanied by an increase in diagnostic accuracy. In bone scanning, this technique would be expected to be fruitful when the activity of different foci of DPD accumulation in the spine has to be compared, e.g., in a patient with back pain to identify the culprit lesion (3, 25). Nevertheless, for bone-SPECT, this assumption has as yet not been systematically investigated in a larger patient group.

The outcome of the phantom study reported here demonstrates the efficiency of CT-based attenuation correction to correct for inhomogeneities in the visualization of tracer distribution caused by attenuation artefacts. It also qualitatively confirms the effect of misregistration between CT and SPECT data on count rates measured on attenuation-corrected SPECT images. However, our data do not lend themselves to prove that CT-based attenuation correction of SPECT data enables quantification of the concentration of radioactivity within the body of patients in absolute terms. For this purpose, the DPD uptake ratios measured would have had to be compared against the real tissue values. Clearly, a more carefully planned phantom study would be needed to fully explore the potential of CT-based attenuation correction in this regard.

Conclusion

- Attenuation correction affects DPD uptake ratios significantly.
- Misalignment between SPECT and CT introduces significant errors in quantification, also affecting left-to-right ratios.

Clinical evaluation of attenuation-corrected scans should therefore be performed carefully; in particular, special attention should be given to possible misalignments between SPECT and CT.

Acknowledgement
The authors thank Ms. Anja Reimann and Mr. Willy Amann for performing the SPECT/spiral-CT studies and other technical support.
The Symbia T2 system was kindly provided by Siemens Medical Solutions.

The support by the ELAN fund of the Medical Faculty of the University of Erlangen/Nürnberg (AZ 04.03.10.1) and by the SFB 603, Teilprojekt C10, financed by the Deutsche Forschungsgemeinschaft is also gratefully acknowledged.
The data published are part of the doctoral thesis of Ms. Valentine Schulz.

References

1. Aizer-Dannon A, Bar-Am A, Ron IG et al. Fused functional-anatomic images of metastatic cancer of cervix obtained by a combined gamma camera and an X-ray tube hybrid system with an illustrative case and review of the ^{18}F-fluorodeoxyglucose literature. Gynecol Oncol 2003; 90: 453–7.
2. Bockisch A, Beyer T, Antoch G et al. Positron emission tomography/computed tomography--imaging protocols, artifacts, and pitfalls. Mol Imaging Biol 2004; 6: 188–99.
3. Case JA, Licho R, King MA et al. Bone SPECT of the spine: A comparison of attenuation correction techniques. J Nucl Med 1999; 40: 604–13.
4. Celler A, Dixon KL, Chang Z et al. Problems created in attenuation-corrected SPECT images by artifacts in attenuation maps: a simulation study. J Nucl Med 2005; 46: 335–43.
5. Cohade C, Osman M, Marshall LN et al. PET-CT: accuracy of PET and CT spatial registration of lung lesions. Eur J Nucl Med Mol Imaging 2003; 30: 721–6.
6. Dresel S, Schwenzer K, Brinkbaumer K et al. ^{18}F-FDG imaging of head and neck tumors: comparison of hybrid PET, dedicated PET and CT. Nuklearmedizin 2001; 40: 172–8.
7. Even-Sapir E, Keidar Z, Sachs J et al.. The new technology of combined transmission and emission tomography in evaluation of endocrine neoplasms. J Nucl Med 2001; 42: 998–1004.
8. Even-Sapir E. Imaging of malignant bone involvement by morphologic, scintigraphic, and hybrid modalities. J Nucl Med 2005; 46: 1356–67.
9. Ficaro EP. Should SPET attenuation correction be more widely employed in routine clinical practice? Eur J Nucl Med Mol Imaging 2002; 29: 409–12.
10. Förster GJ, Laumann C, Nickel O et al. SPET/CT image co-registration in the abdomen with a simple and cost-effective tool. Eur J Nucl Med Mol Imaging 2003; 30: 32–9.
11. Fricke E, Fricke H, Weise R et al. Attenuation correction of myocardial SPECT perfusion images with low-dose CT: Evaluation of the method by comparison with perfusion PET. J Nucl Med 2005; 46: 736–44.
12. Fricke H, Fricke E, Weise R et al. A method to remove artifacts in attenuation-corrected myocardial perfusion SPECT introduced by misalignment between emission scan and CT-derived attenuation maps. J Nucl Med 2004; 45: 1619–25.
13. Gregory PL, Batt ME, Kerslake RW et al. The value of combining single photon emission computerised tomography and computerised tomography in the investigation of spondylolysis. Eur Spine J 2004; 13: 503–9.
14. Groves AM, Bird N, Tabor I et al. 16-Detector multislice CT-skeletal scintigraphy image co-registration. Nucl Med Commun 2004; 25: 1151–5.
15. Hendel RC. Attenuation correction: eternal dilemma or real improvement? Q J Nucl Med Mol Imaging 2005; 49: 30–42
16. Horger M, Eschmann SM, Pfannenberg C et al. Evaluation of combined transmission and emission tomography for classification of skeletal lesions. AJR Am J Roentgenol 2004; 183: 655–61.
17. Keidar Z, Israel O, Krausz Y. SPECT/CT in tumor imaging: technical aspects and clinical applications. Semin Nucl Med 2003; 33: 205–18.
18. Kim JH, Czernin J, Allen-Auerbach MS et al. Comparison between ^{18}F-FDG PET, in-line PET/CT, and software fusion for restaging of recurrent colorectal cancer. J Nucl Med 2005; 46: 587–95.
19. Matsunari I, Böning G, Ziegler SI et al. Effects of misalignment between transmission and emission scans on attenuation-corrected cardiac SPECT. J Nucl Med 1998; 39: 411–6.
20. Moreira AP, Duarte LH, Vieira F et al. Value of SPET/CT image fusion in the assessment of neuroendocrine tumours with ^{111}In-pentetreotide scintigraphy. Rev Esp Med Nucl 2005; 24: 14–8.
21. Nakamoto Y, Tatsumi M, Cohade C et al. Accuracy of image fusion of normal upper abdominal organs visualized with PET/CT. Eur J Nucl Med Mol Imaging 2003; 30: 597–602.
22. Nömayr A, Römer W, Hothorn T et al. Anatomical accuracy of lesion localization. Retrospective interactive rigid image registration between ^{18}F-FDG-PET and X-ray CT. Nuklearmedizin 2005; 44: 149–55.
23. Nömayr A, Römer W, Strobel D et al. Anatomical accuracy of hybrid SPECT/spiral CT in the lower spine. Nucl Med Commun 2006; 27: 521–8.
24. Pfannenberg AC, Eschmann SM, Horger M et al. Benefit of anatomical-functional image fusion in the diagnostic work-up of neuroendocrine neoplasms. Eur J Nucl Med Mol Imaging 2003; 30: 835–43.
25. Römer W, Beckmann MW, Forst R et al. SPECT/Spiral-CT hybrid imaging in unclear foci of increased bone metabolism: a case report. Rontgenpraxis 2005; 55: 234–7.
26. Römer W, Fiedler E, Pavel M et al. Attenuation correction of SPECT images based on separately performed CT: Effect on the measurement of regional uptake values. Nuklearmedizin 2005; 44: 20–8.
27. Römer W, Nömayr A, Uder M et al. SPECT-guided CT for evaluating foci of increased bone metabolism classified as indeterminate on SPECT in cancer patients. J Nucl Med 2006; 47: 1102–6.
28. Römer W, Reichel N, Vija HA et al. Isotropic reconstruction of SPECT data using OSEM3D: correlation with CT. Acad Radiol. 2006; 13: 496–502.
29. Schillaci O, Danieli R, Manni C et al. Is SPECT/CT with a hybrid camera useful to improve scintigraphic imaging interpretation? Nucl Med Commun 2004; 25: 705–10.
30. Schillaci O, Simonetti G. Fusion imaging in nuclear medicine-applications of dual-modality systems in oncology. Cancer Biother Radiopharm 2004; 19: 1–10.
31. Schillaci O, Spanu A, Madeddu G. ^{99m}Tc-sestamibi and ^{99m}Tc-tetrofosmin in oncology: SPET and fusion imaging in lung cancer, malignant lymphomas and brain tumors. Q J Nucl Med Mol Imaging 2005; 49: 133–44.
32. Schillaci O. Functional-anatomical image fusion in neuroendocrine tumors. Cancer Biother Radiopharm 2004; 19: 129–34.
33. Schillaci O. Hybrid SPECT/CT: a new era for SPECT imaging? Eur J Nucl Med Mol Imaging 2005; 32: 521–4.
34. Stodilka RZ, Kemp BJ, Prato FS et al. Importance of bone attenuation in brain SPECT quantification. J Nucl Med 1998; 39: 190–7.
35. Tang HR, Brown JK, Da Silva AJ et al. Implementation of a combined CT scintillation camera system for localizing and measuring radionuclide uptake: experiments in phantoms and patients. IEEE Trans Nucl Sci 1999: 46: 551–7.
36. Tatsch K, Asenbaum S, Bartenstein P et al. European Association of Nuclear Medicine Procedure Guidelines for Brain Perfusion SPET using ^{99m}Tc-labelled radiopharmaceuticals. Eur J Nucl Med Mol Imaging 2002; 29: BP36-42.
37. Tharp K, Israel O, Hausmann J et al. Impact of ^{131}I-SPECT/CT images obtained with an integrated system in the follow-up of patients with thyroid carcinoma. Eur J Nucl Med Mol Imaging 2004; 31: 1435–42.
38. Townsend DW, Beyer T, Blodgett TM. PET/CT scanners: a hardware approach to image fusion. Semin Nucl Med 2003; 33: 193–204.
39. Utsonomiya D, Shiraishi S, Imuta M et al. Added value of SPECT/CT fusion in assessing suspected bone metastasis: comparison with scintigraphy alone and nonfused scintigraphy and CT. Radiology 2006; 238: 264–71.
40. Zaidi H, Hasegawa B. Determination of the attenuation map in emission tomography. J Nucl Med 2003; 44: 291–315.

Correspondence to:
Torsten Kuwert, MD
Clinic of Nuclear Medicine, University of Erlangen/ Nürnberg
Krankenhausstr. 12, 91054 Erlangen, Germany
Tel. +49/(0)91 31/8 53–34 11, Fax –92 62
E-mail: torsten.kuwert@nuklear.imed.uni-erlangen.de